Piezochromic Effect and Orientational Order in Monolayers and LB Multilayers of Poly(*p*-phenylenesulfonate)−Dioctadecyldimethylammonium Bromide Complexes

Joachim Engelking,[†] Dagmar Ulbrich,[‡] and Henning Menzel*,[†]

Institut für Makromolekulare Chemie der Universität Hannover, Am Kleinen Felde 30, D-30167 Hannover, Germany, and Max-Planck-Institut für Polymerforschung, Ackermannweg 10, D-55128 Mainz, Germany

Received May 11, 2000; Revised Manuscript Received September 21, 2000

ABSTRACT: By spreading dioctadecyldimethylammonium bromide (DODA) on a subphase containing rigid-rod-like poly(*p*-phenylenesulfonate)s (PPPS), polyelectrolyte complexes are formed in situ at the air−water interface. These complex monolayers are investigated by recording surface pressure/area isotherms, UV/vis spectroscopy, and, after transfer onto a solid substrate, X-ray photoelectron spectroscopy (XPS) and X-ray reflectivity (XR). XPS and XR measurements indicate that although the polyelectrolytes are aggregated in aqueous solution, the complexes are stoichiometric. The isotherms show that the area per amphiphile in the complex monolayer is significantly higher than in the monolayer of pure DODA. This is due to the distance of the ionic sites along the rigid-rod-like polymer chain and results in a more tilted arrangement of the alkyl chains as confirmed by the XR measurements. UV/vis spectroscopy reveals that the A-band of the PPPS is red-shifted in the complex, and a further red shift of the A-band upon compression of the complex monolayer is observed. This two-dimensional piezochromic effect is discussed to be a result of the electronic interaction of the π-systems, which improves with decreasing distance during compression. Upon transfer to solid substrates the rigid-rod-like polyelectrolytes are oriented to be parallel to the dipping direction as evidenced by polarized UV/vis spectroscopy. The degree of order in the LB film shows a linear dependence on the axial ratio of the rigid-rod-like PPPS.

Introduction

Polyelectrolytes and oppositely charged amphiphiles form stable complexes which have remarkable properties.[1] In particular, they exhibit interesting solid-state morphologies due to the separation of the ionic sites and the hydrophobic parts[2,3] and have found application in surface coatings, drug release systems, etc.[1,2] Such complexes are typically obtained by mixing aqueous solutions of the polyelectrolyte and the amphiphile. However, polyelectrolyte−amphiphile complexes also can be formed by spreading an amphiphile solution on an aqueous subphase containing the polyelectrolyte.[4,5] This complex formation between a monolayer at the air/water interface and a polyelectrolyte dissolved in the subphase provides a versatile way to combine in thin films the properties of water-soluble polyelectrolytes and ionic amphiphiles.[6] This method was previously used to increase the monolayer stability, thus enabling monolayer transfer,[4,5,7] to adjust the area per azobenzene amphiphile, thus enabling photoisomerization,[8−11] and to control membrane permeability.[12,13] These effects rely on structural changes in the monolayer upon adsorption of the polyelectrolyte to the monolayer and subsequent complex formation. The structural changes occurring upon polyelectrolyte adsorption can be used to monitor the adsorption process when a preformed monolayer of ionic amphiphiles is brought into contact with a subphase containing an oppositely charged polyelectrolyte.[14−18]

The properties of poly(*p*-phenylene)s may be applicable for advances in light-emitting diodes. Oriented films of poly(*p*-phenylene)s are of particular interest in this respect, because of their polarized emission.[19] It was previously demonstrated that complexation of a cationic poly(*p*-phenylene) with a fluorinated amphiphile significantly increases the fluorescence intensity.[20] Furthermore, poly(*p*-phenylenes) are rigid-rod-like and as such have been used to study the behavior of polyelectrolytes. The advantage of these compounds is that the chain geometry is largely fixed by the chemical structure. As a result, changes of shape induced by solvation and coulomb interactions are unlikely.[21,22] In addition, rigid rods are expected to form a two-dimensional nematic phase when adsorbed to a surface.[23] Therefore, interesting effects due to the ordering of the polymer chains are expected for complexes of rigid-rod-like polyelectrolytes at the air/water interface.

In this paper we describe studies to elucidate the structure and properties of complexes of poly(*p*-phenylenesulfonates) (PPPS, PPPX) of different molecular weight with dioctadecyldimethylammonium bromide (DODA) (see Scheme 1). These complexes are further compared to complexes of DODA with flexible anionic polyelectrolytes like poly(styrenesulfonate) (PSS) or poly(vinyl sulfonate) (PVS). The monolayer structure is examined by recording surface area/pressure isotherms and by UV/vis spectroscopy. These investigations are complemented by UV/vis spectroscopy, X-ray photoelectron spectroscopy (XPS), and X-ray reflectivity measurements (XR) on Langmuir−Blodgett (LB) multilayers fabricated from the complex monolayers.

Experimental Section

Poly(phenylenesulfonate)s PPPS and PPPX were synthesized and characterized as described previously.[21,24] Molecular

---

[†] Institut für Makromolekulare Chemie der Universität Hannover.

[‡] Max-Planck-Institut für Polymerforschung.

* Corresponding author. Fax +49 511 762 4996, E-mail Menzel@mbox.imc.uni-hannover.de.

10.1021/ma0008140 CCC: $19.00

Scheme 1

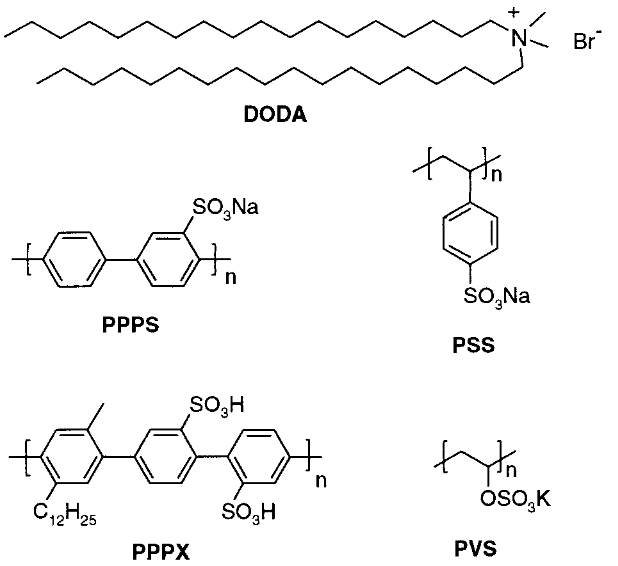

Scheme 2

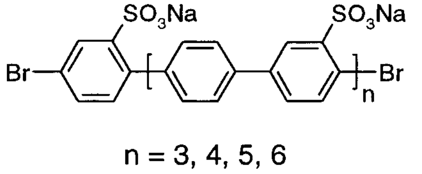

Table 1. Degree of Polymerization $\bar{P}_n$ and Polydispersity ($\bar{M}_w/\bar{M}_n$) of Poly(*p*-phenylenesulfonates) As Determined by GPC Employing the Universal Calibration Reported by Vanhee et al.[25]

polymer	$\bar{P}_n$	$\bar{M}_w/\bar{M}_n$
PPPS(4)[a]	7[b]	1.3
PPPS(23)	23	1.5
PPPS(36)	36	2.1
PPPS(54)	54	4.5
PPPX	16	2.3

[a] The numbers give the average degree of polymerization. [b] P_n determined by MALDI-TOF is 4.

weights were determined for the corresponding precursor polymers via GPC (THF) using the universal calibration for substituted poly(*p*-phenylenes) reported by Vanhee et al.[25] The degree of polymerization and the polydispersity are listed in Table 1.

The molecular weight distribution of the oligomer PPPS(4) in the precursor form was also investigated by means of MALDI-TOF using a Bruker Reflex instrument, equipped with a nitrogen laser. The sample preparation is described in ref 26. 1,3,7-Trihydroxyanthracene (dithranol) was used as the matrix material. The predominating species of PPPS(4) determined by mass spectrometry is shown in Scheme 2 where *n* is 3, 4, 5, or 6. In further discussion the number-average degree of polymerization determined by MALDI-TOF ($\bar{P}_n = 4$) will be used to designate the oligomer.

Poly(sodium-*p*-styrenesulfonate) (PSS) ($\bar{M}_w$ about 100 000 g/mol, Acros), poly(potassium vinyl sulfate) (PVS) ($\bar{M}_w$ about 170 000 g/mol, Aldrich), and dioctadecyldimethylammonium bromide (DODA) (>99%, Selectophore, Fluka) were used as received. Monolayers were investigated using a Nima 611MC (300 cm^2) trough equipped with a Wilhelmy plate pressure sensor Nima PS4. Monolayers were prepared by spreading a solution of the amphiphile in chloroform on a subphase of ultrapure water (>18 MΩ·cm, Barnstaedt NanopureIII, 20 °C) containing the polyelectrolyte (concentration 5×10^{-5} mol/L with respect to the anionic groups). After spreading, evaporation of chloroform and complex formation occurred for 15 min before recording the isotherms. The isotherms were recorded with a barrier speed corresponding to an area decrease of 10 cm^2/min. The monolayers were transferred onto hydrophobic quartz slides and silicon wafers at a surface pressure of 35 mN/m and a dipping speed of 10 mm/min. To avoid defects due to partial removal, the film was allowed to dry for 10 min before the next dipping. The setup and procedure for recording the monolayer UV/vis spectra have been reported in ref 27. The preparation of substrates as well as the UV/vis spectroscopy of Langmuir−Blodgett (LB) films is described in ref 28. X-ray photoelectron spectra were obtained on a ESCA 5600CI (Physical Electronics) using monochromatic Al Kα radiation at a takeoff angle of 45°. X-ray reflectometry was performed using a Siemens D500 diffractometer in the reflection mode (Ni-filtered Cu Kα radiation, $\lambda = 1.542$ nm).

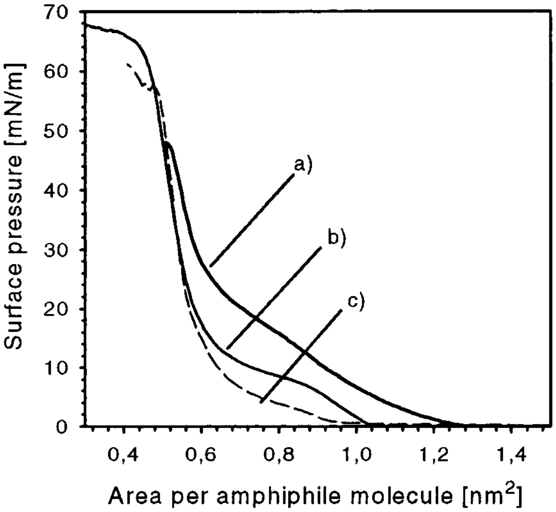

Figure 1. Surface pressure/area isotherms for DODA spread on (a) pure water and on subphases containing (b) PSS and (c) PVS ($c_{\text{ionic groups}} = 5 \times 10^{-5}$ mol/L).

Results and Discussion

Surface Pressure/Area Isotherms. The isotherms of DODA spread on pure water and of the complexes obtained by spreading DODA on subphases containing polyelectrolytes are significantly different. The isotherm of DODA on pure water (see Figure 1) shows two regions.[29−31] The first increase in surface pressure occurs at an area of approximately 1.25 nm^2 per amphiphile, and the high area per molecule indicates an expanded monolayer structure. A second region is evident at a surface pressure of approximately 20 mN/m as this monolayer adopts a more condensed structure.[32] The area per molecule for the densely packed structure is determined by extrapolation to be 0.68 nm^2. This area per DODA amphiphile is significantly higher than expected for a dense arrangement of two alkyl chains (ca. 0.40 nm^2). The high area per molecule in the film cannot be explained solely by the coulomb repulsion of the ionic headgroups and their hydration shell.[32] From single crystal investigations on DODA, it is known that the steric crowding at the nitrogen atom allows only one of the two alkyl chains to be all-trans. The second alkyl chain adopts several gauche conformations in the vicinity of the headgroup. Therefore, the alkyl chains in single crystals adopt a tilted arrangement, and the area per DODA molecule is 0.56 nm^2.[33]

For complexes with flexible anionic polyelectrolytes such as poly(styrenesulfonate) (PSS) or poly(vinyl sulfonate) (PVS) a different monolayer behavior is observed[6] (Figure 1). The phase transition occurs at a

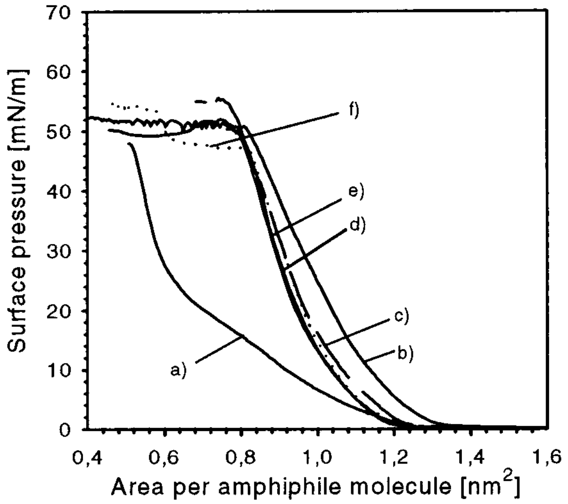

Figure 2. Surface pressure/area isotherms for DODA spread on (a) pure water and on subphases containing (b) PPPS(4), (c) PPPS(23), (d) PPPS(36), (e) PPPS(54), and (f) PPPX ($c_{\text{ionic groups}} = 5 \times 10^{-5}$ mol/L).

Table 2. Area Per Amphiphile at Zero Pressure A_0, Area Per Amphiphile at the Collapse A_c, and Collapse Pressure Π_c for DODA on Pure Water and on Subphases Containing Anionic Polyelectrolytes

polyelectrolyte	A_0 [nm^2]	A_c [nm^2]	Π_c [mN/m]
none	0.68	0.52	48
PSS	0.61	0.46	65
PVS	0.60	0.49	57
PPPS(54)	1.02	0.79	51
PPPX	1.06	0.82	47

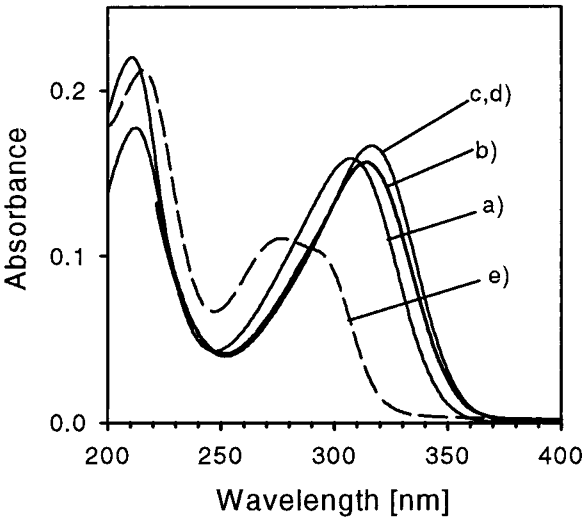

Figure 3. UV/vis spectra of (a) PPPS(4), (b) PPPS(23), (c) PPPS(36), (d) PPPS(54), and (e) PPPX in aqueous solution normalized to 10^{16} phenylene units.

significantly reduced surface pressure, and the area per DODA amphiphile is reduced to 0.61 and 0.60 nm^2, respectively,[6,34] which are close to the value found in single crystals (0.56 nm^2).[33] The lower area per amphiphile in the complex monolayer compared to the monolayer on pure water can be ascribed to the charge compensation, which significantly reduces the Coulombic interaction of the headgroups.

The situation is completely different for the complexes with the anionic poly(*p*-phenylene)s (PPPS and PPPX) (Figure 2). For both polyelectrolytes the area per amphiphile in the complex is significantly larger than for the amphiphile on pure water (Table 2). Furthermore, the isotherms for the complex monolayers with the anionic poly(*p*-phenylene)s do not have a plateau that indicates a change in the monolayer structure during the compression. The difference in the area per amphiphile can be explained by the differences in charge density and flexibility of the polymers. For PPPS, the ionic sites are directly bound to the rigid polymer backbone, while they are linked to a flexible chain via a phenyl group "spacer" in PSS. The distance between the charges is therefore very flexible in the case of PSS (0.25−1.2 nm). As a result, the ionic groups in the complex can adjust their distance according to the distance of the ionic amphiphile headgroups. However, in the case of PPPS the distance between the charges is fixed due to the rigid *p*-phenylene structure and can be calculated to be 0.9−1.1 nm.

In a stoichiometric DODA/PPPS complex there are two phenylene rings for every amphiphile, resulting in an area per phenylene ring of 0.51 nm^2. This value is in agreement with literature reports. Vahlenkamp has investigated uncharged poly(*p*-phenylene)s with alkoxy side chains and reports an area per phenylene ring of 0.30−0.40 nm^2. The former value however was determined for rather unstable monolayers, for which a partial collapse cannot be ruled out.[35] The tetrabutylammonium salt of PPPS however gives an area per phenylene ring of 0.55 nm^2.[21] Charged poly(*p*-phenylene) derivatives were also investigated by Ulbrich. These derivatives give an area per phenylene unit of 0.40−0.55 nm^2.[36] PPPX has a higher charge density than PPPS (two sulfonate groups per three phenylene rings), which should result in a lower area per amphiphile. However, a very similar area per amphiphile is measured for the PPPX and PPPS complexes. This is explained by the fact that the PPPX has additional alkyl substituents, which also contribute to the area requirements. Therefore, in the case of a stoichiometric PPPX complex 1.5 phenylene units (1.5 × 0.5 nm^2) and 1 alkyl chain (0.2 nm^2) per amphiphile contribute to an estimated area of 0.95 nm^2, which is close to the experimental value (1.06 nm^2).

For PPPS a significant influence of the molecular weight on the monolayer properties of the resulting DODA complex is observed (Figure 2). The lower the molecular weight, the higher the area per amphiphile in the complex (1.02 nm^2 for $\bar{P}_n = 54$ and 1.17 nm^2 for $\bar{P}_n = 4$). The effect is particular pronounced for the oligomeric PPPS(4). This trend may be related to an increase in defects in the monolayer structure caused by the increasing number of end groups. A similar observation has been described for complexes of a double chain ammonium amphiphile and PSS with various degrees of polymerization ($\bar{P}_n = 50-2400$).[37]

UV/vis Spectroscopy. UV/vis spectroscopy is a valuable tool for the investigation of poly(*p*-phenylene)s. These polymers typically have two absorption bands.[38,39] The so-called B-band ($\lambda_{\max} \sim 200$ nm) corresponds to electronic transitions between localized orbitals of the phenylene units, and the A-band ($\lambda_{\max} > 300$ nm) is due to transitions between delocalized orbitals. For nonsubstituted poly(*p*-phenylene)s the absorption maxima of the A-band depends on the number of phenylene units. For large numbers of phenylene units, in which the maximum conjugation length is exceeded, $\lambda_{\max}$ has been calculated to be 339[40] or 344 nm.[41] The effective conjugation length is significantly reduced by the pres-

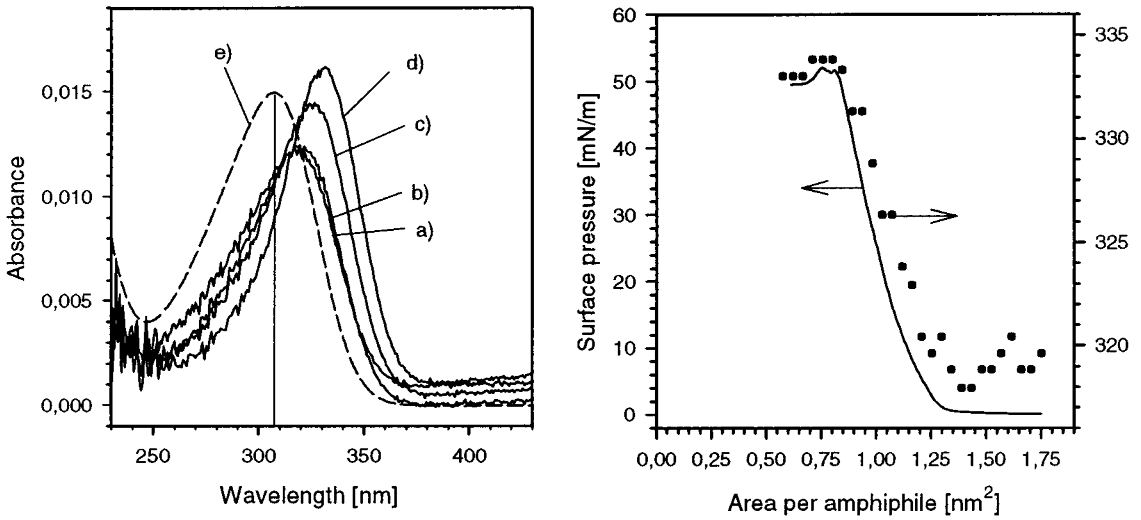

Figure 4. UV/vis spectra of PPPS(4)/DODA complex monolayers at (a) 1.71 nm^2, 0 mN/m, (b) 1.25 nm^2, 2.7 mN/m, (c) 1.07 nm^2, 16 mN/m, (d) 0.94 nm^2, 34.3 mN/m, and (e) in solution (different scaling) (left) and wavelength at the peak maximum (λ_{max}) as a function of the area per amphiphile.

Table 3. Spectroscopic Data for Poly(*p*-phenylene)s in Solution, as a Complex Monolayer, and as a LB Film, as Well as the Two-Dimensional Order Parameter S_{xy} and Transfer Ratio for the LB Films

	λ_{max} [nm]					
polymer	solution in water	monolayer $\Pi \sim 0$ mN	monolayer $\Pi \sim 50$ mN	LB film[a]	$S_{xy} \pm 0.02$	transfer ratio (%)
PPPS(4)	308	319	334	328	0.14	92
PPPS(23)	313			330	0.18	88
PPPS(36)	317			330	0.32	95
PPPS(54)	317	321	334	330	0.39	95
PPPX(16)	275	295	295	295	0.37	88

[a] Transferred at 35 mN/m.

ence of substituents, because they cause a twist of the phenylene units. This induces a blue shift in the A-band for substituted poly(*p*-phenylene)s. In the case of large twists the A-band may be almost completely suppressed as is the case for poly(2,4-dialkyl-*p*-phenylene)s.[17,42,43] For PPPS the twist is not as pronounced, resulting in an A-band at 317 nm in solution (see Figure 3c). For the oligomeric PPPS(4) the A-band is blue shifted to 308 nm (see Figure 3a), because the average chain length is smaller than the maximum conjugation length, which has been determined to comprise 9−11 phenylene units.[35] Aqueous solutions of PPPX exhibit an A-band with a maximum around 280 nm (see Figure 3e). The blue shift of the PPPX A-band compared to the A-band of PPPS is due to the additional alkyl chains which may induce a twist. The shape of the peak suggests that the band is a convolution of two components.

For all investigated poly(*p*-phenylenesulfonate) complex monolayers with DODA, the A-band is red-shifted compared to the corresponding solutions (Figure 4). Upon compression of the monolayer, the peak absorbance increases and the peak is shifted even further. The peak shift reaches a maximum just before the collapse of the monolayer. In addition, there is no further peak shift (Figure 4) or even a partial reversal upon collapse of the monolayer.[6] The peak shift can also be observed by investigating LB films fabricated from the monolayers. The peak position in the LB film corresponds exactly to the peak position in the monolayer at the air/water interface at the transfer pressure. All peak positions determined for monolayers at the air/water interface or for LB films are summarized in Table 3.

The increase of the peak height upon compression is due to the increased number of detected chromophores in the illuminated area. However, the peak shift is a pressure induced process as observed for polysilane monolayers by Yoshida et al.[44] The authors termed the effect “two-dimensional piezochromism”. It is worth noting that the “piezochromic” effect in the case of the PPPS/DODA complex monolayer results in the same final peak position for high molecular weight PPPS(54)[6] and for oligomeric PPPS(4) (Figure 4). That is, the peak position for the compressed complex monolayer does not depend on the degree of polymerization as was the case for the peak position for PPPS in solution. There are several possible explanations for the peak shift upon complexation and compression of the PPPS/DODA monolayers, namely (i) solvatochromic effects, (ii) charge compensation, i.e., electronic effects, (iii) steric effects caused by the complexation with ammonium groups, (iv) $\pi-\pi$ interaction of the chromophores, or (v) planarization of the polymer backbone, resulting in a larger effective conjugation length.

When changing the environment for the poly(phenylene) from a highly polar solvent (water) to a less polar environment (monolayer), solvatochromic effects could cause a peak shift. To elucidate these influences, the absorption spectra of PPPS(4) for different solvent compositions (Table 4) were investigated. Dissolved in pure water, PPPS(4) has a peak maximum at 308 nm, and addition of polar solvents like methanol or ethanol or of less polar solvents like dioxane and THF (dielectric constants at RT: water, 80.4; methanol, 33.6; ethanol, 24.3; dioxane, 2.21; THF, 7.47[45,46]) results only in a small red shift of ca. 3 nm. Therefore, a solvatochromic effect can be excluded as a major contribution for the peak shift in the PPPS/DODA monolayers.

Table 4. Influence of the Solvent and of the Addition of Tetrabutylammonium Iodide (TBA) and Sodium Chloride, Respectively, on the Position of the A-Band of PPPS(4) (cPPPS = 10 mg/L, at RT)

solvent	$\lambda_{\max}$ [nm]	solvent	$\lambda_{\max}$ [nm]
water	308.0	TBA (2 equiv)	310.5
water/methanol(1:1)	308.0	TBA (20 equiv)	315.0
water/ethanol (1:1)	308.0	TBA (40 equiv)	315.5
water/dioxane (1:1)	311.5	NaCl (20 equiv)	310.0
water/THF (1:1)	311.5		

The addition of a tetrabutylammonium salt (TBA) in high excess, as a model for the amphiphile headgroup, on the other hand, results in a significant red shift of 7 nm (Table 4). So, it can be conjectured that the complexation of the PPPS backbone with ammonium groups contributes to the peak shift for complex monolayers. Lower concentrations of TBA and/or the addition of sodium chloride (even in high excess) show only minor effects. Therefore, it can be concluded that the peak shift upon complexation with the ammonium headgroup is rather a steric effect on the PPPS backbone than an electronic effect due to charge compensation. However, the complexation with TBA might also result in a less soluble species which forms larger aggregates with improved $\pi-\pi$ interaction. Although the steric effect of the complexation with the ammonium headgroups may contribute to the peak shift observed for the monolayer, it cannot explain the piezochromic effect. Thus, improved $\pi-\pi$ interaction or planarization caused by the surface pressure must be considered in order to explain the further peak shift upon compression.

The piezochromic effect observed for the polysilanes was explained by a pressure-induced transformation of the polymer into an all-trans configuration resulting in better σ-conjugation.[44] A strong red shift of the A-band and additional bands have also been found for alkyl-substituted poly(thiophene)s in LB and spin-coated films and were attributed to a planarization of the polymer backbone.[47] The shape and maximum of the A-band of conjugated aromatic or heteroaromatic polymers can also be shifted by the formation of aggregates. For poly(fluorene) derivatives, Bradley et al. found aggregation in certain solvents which is accompanied by the occurrence of a new band in the spectrum.[48] Similar results have been described by Fiesel et al. for an alkyl-substituted poly(*p*-phenylene−ethinylene) and have been rationalized with a parallel arrangement of the polymer chain in the aggregates.[49] In such an arrangement the π-systems of neighboring polymer chains can interact, shifting the UV absorption band. The effect is comparable to the well-investigated[50−52] and well-understood[53] band shift of aggregated azobenzene derivatives.

Both the planarization of the polymer backbone, which results in a larger effective conjugation length, and the improved $\pi-\pi$ interaction of the chromophores require a well-organized arrangement of the polymer chains parallel to each other. At low surface pressure the polymer chains are already parallel to the water surface in order to maximize the interactions with the oppositely charged amphiphile monolayer. Therefore, a peak shift relative to the solution will occur. Increasing the surface pressure reduces defects, brings the polymer chains very close together, and therefore further shifts the peak. The peak shift is partially reverted at the collapse, because the collapse is accompanied by a partial structure relaxation. So both mechanisms can be used to explain the peak shift upon complexation and the piezochromic effect. However, there is some experimental data that indicate that $\pi-\pi$ interaction of the poly(*p*-phenylene) chains is predominant for the piezochromic effect. If the peak shift were due only to a planarization of the polymer backbone, the final peak position for PPPS(54) should be different from that of PPPS(4), because in the latter case the number of connected phenylene rings is lower than the maximum effective conjugation length. Another indication that the improved $\pi-\pi$ interaction is causing the piezochromic effect is the fact that the PPPX/DODA complex monolayer shows a peak shift upon complexation, without a corresponding piezochromic effect (Table 3). This can be explained by the additional alkyl chains present in PPPX which do not allow the polymer chains to come close enough for effective $\pi-\pi$ interaction even if a surface pressure is applied.

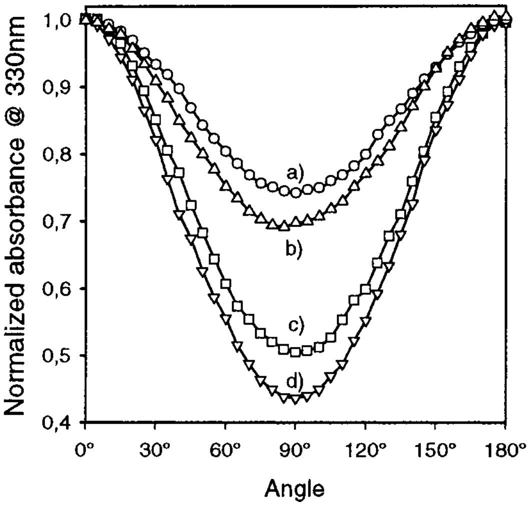

Figure 5. Normalized absorbance at 330 nm for PPPS/DODA complex LB films as a function of the angle between the polarizer and the dipping direction: (a) PPPS(4), (b) PPPS(23), (c) PPPS(36), and (d) PPPS(54).

Orientational Order. The orientational order of the poly(*p*-phenylene) chains in the LB films can be investigated by polarized UV/vis spectroscopy because the transition dipole of the A-band is oriented along the main molecular axis. The A-band shows significant anisotropy for the PPPS/DODA complex LB films, indicating a high degree of orientational order. The absorbance at 330 nm as a function of the angle between polarizer and dipping direction can be used as a measure for the orientational order (Figure 5). According to Schwiegk et al., for LB films of rigid-rod-like polymers a two-dimensional order parameter S_{xy} can be defined as[54]

$$S_{xy}^{\lambda} = \frac{A_{\parallel} - A_{\perp}}{A_{\parallel} + A_{\perp}}$$

with $A_{\parallel}$ and $A_{\perp}$ being the absorbance parallel and perpendicular to the preferred direction, respectively.

As has been shown, the orientational order in LB films of “hairy rod”-like polymers is due to a flow-induced orientation of the two-dimensional liquid crystalline domains in the monolayer.[54−56] The occurrence of orientational order in the PPPS/DODA system therefore indicates that the complex behaves like a “hairy rod” system and forms two-dimensional liquid crystalline domains at the air−water interface.

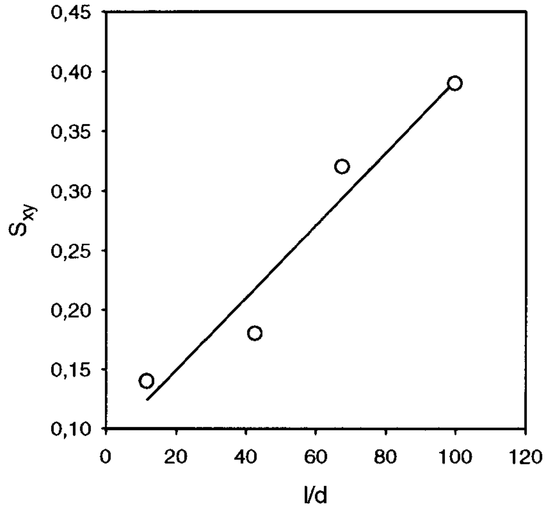

Figure 6. Two-dimensional order parameter S_{xy} as a function of the ratio of rod length to rod diameter *l*/*d* for PPPS/DODA complex LB films.

For PPPS(54)/DODA LB films the two-dimensional order parameter ($S_{xy} = 0.39$) is similar to other "hairy rod"-like systems.[54–56] The order parameter S_{xy} decreases significantly with decreasing degree of polymerization (Table 3). In fact, for the range of molecular weights investigated here, a linear dependence of the order parameter on the axial ratio *l*/*d* is observed (Figure 6). It can be conjectured that the liquid crystalline order in the monolayer domains depends on the axial ratio of the rods, as is the case for melts of rigid rods.[57,58]

Complex Stoichiometry and Complex Structure. PPPS and PPPX are both known to form aggregates in aqueous solutions.[59] The aggregates form independently of the molecular weight of the polymer and are in equilibrium with molecular dispersed polymer chains.[60,61] The PPPX aggregates have a radial aggregation number of seven and a diameter of approximately 3.7 nm, while PPPS aggregates have a radial aggregation number of 4 and a diameter of 2.2 nm.[59] The formation of aggregates is due to the rigid-rod-like structure and the amphiphilic nature of the polymers, which are bearing ionic sites as well as hydrophobic groups.[59–61]

The questions arises whether complexes with the DODA amphiphiles are formed by adsorption of significant amounts of intact aggregates, by adsorption of aggregates and subsequent disruption of the aggregates, or by adsorption of molecular dispersed polyelectrolyte chains. To address this question, we have determined the complex stoichiometry in the LB films by X-ray photoelectron spectroscopy (XPS).[6] Although the precision of XPS measurements is limited, it is sufficient to detect the adsorption of significant amounts of intact aggregates.[62] In the case of adsorption of intact aggregates, a significant surplus of sulfur is expected. However, XPS spectra recorded for the PPPS/DODA complexes[6] and the PPPX/DODA complexes indicate 1:1 stoichiometry (Table 5). Furthermore, the survey scans do not show any signals indicating significant amounts of sodium ions (see Figure 7). The survey scan does not include the region below 100 eV, where the Br signals would occur. However, even in the case of a nonstoichiometric complex, no significant amounts of Br$^-$ can be expected. When DODA is spread at the air/water interface, the Br$^-$ counterions are dissolved in the subphase, but Br$^-$ concentration in the subphase is negligible since the amount of amphiphile spread is so small. Therefore, the main counterion for the amphiphile is the OH$^-$ ion.[32] The XPS measurements therefore support the adsorption of molecular dispersed polymer chains to the monolayer or a disruption of the aggregates upon complexation.

Table 5. Complex Stoichiometry As Determined by XPS and Comparison to the Theoretical Values for 1:1 Stoichiometric Complexes

	DODA/PPPS(23)		DODA/PPPX	
	exp [%]	theor (1:1) [%]	exp [%]	theor (1:1) [%]
C (C 1s)	90.8	90.9	89.2	91.3
O (O 1s)	5.7	5.4	6.1	5.2
S (S 2s)	1.7	1.8	1.5	1.7
N (N 1s)	1.7	1.8	1.5	1.7

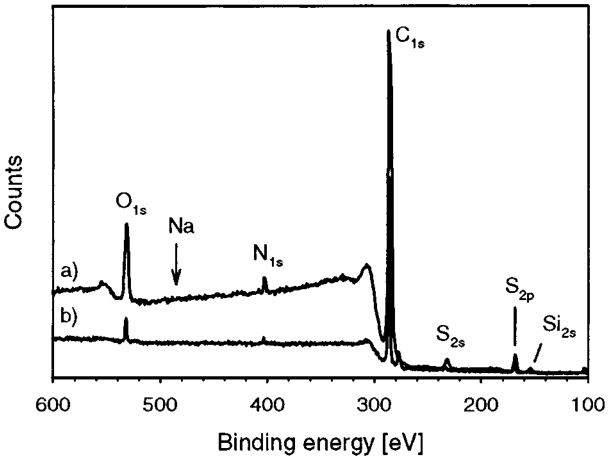

Figure 7. XPS survey scans for LB films of (a) PPPS(23)/DODA (26 layers) and (b) PPPX/DODA (28 layers).

Compared to the single polymer chain, the aggregates have a significantly larger diameter. If aggregates are adsorbed to the monolayer, the large diameter should result in a significantly larger layer thickness or a distorted layer structure of the LB films. Therefore, investigation of complex LB films via X-ray reflectometry should reveal additional information about the presence of aggregates in the complex. X-ray reflection curves for LB films of the PPPS(4)/DODA, PPPS(36)/DODA, and PPPX/DODA were recorded, and all show Kiessig fringes and Bragg peaks (Figure 8). From the Bragg peaks a double-layer thickness of 3.1 nm is calculated. The occurrence of Kiessig fringes up to large *q* values is an indication of a well-defined layer structure and small roughness of the overall film.[63] Therefore, significant amounts of aggregated PPPS in the PPPS/DODA complex can be excluded.

For the PPPX/DODA complex LB film there are Bragg peaks as well. However, the film is somewhat rougher as indicated by the smaller number of Kiessig fringes. Furthermore, the thickness of the double layer is slightly higher compared to the PPPS/DODA complex (Table 6). The slightly higher layer thickness can be explained by an insertion of the alkyl chain substituents into the amphiphile monolayer, while the higher roughness of the film is caused by the transfer properties of the PPPX/DODA complex. Even under optimized conditions, the transfer rates were only approximately 88%. Therefore, the presence of significant amounts of aggregates in the complex monolayer is unlikely for the PPPX/DODA system as well.

The double-layer thickness for LB films of DODA was reported to be 4.3 nm.[64] Using this double-layer thick-

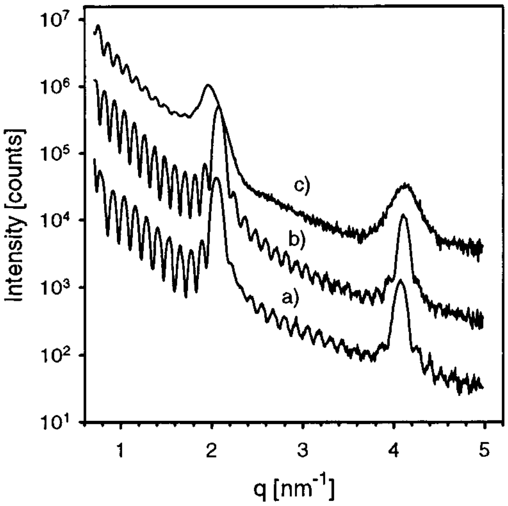

Figure 8. X-ray reflectivity for LB films of (a) PPPS(4)/DODA (32 layers), (b) PPPS(36)/DODA (36 layers), and (c) PPPX/DODA (36 layers).

Table 6. Layer Thickness and Approximate Tilt Angle for LB Films of PPPS/DODA and PPPX/DODA Complexes As Determined by X-ray Reflectivity (Transfer at 35 mN/m) and Comparison with Literature[4,64]

system	d (double layer) [nm]	approx tilt angle φ [deg]
PPPS(4)/DODA	3.08 ± 0.01	50
PPPS(36)/DODA	3.05 ± 0.01	50
PPPX/DODA	3.09−3.26	50
DODA[64]	4.3	30
PSS/DODA[4,64]	4.2−4.3	30

ness and the calculated length for the extented amphiphile chain (ca. 2.50 nm), the tilt angle φ can be calculated to be about 30°.[64] The double-layer thickness for LB films of PSS/DODA complex is reported to be 4.2−4.3 nm as well.[64,65] That is, the polyelectrolyte chain does not contribute significantly to the double-layer thickness. As already mentioned, for PPPS/DODA and PPPX/DODA complex LB films the double layer is significantly thinner (3.1−3.3 nm). This change in thickness is explained by the larger area per amphiphile in the monolayer. To compensate for the higher areal requirements, the alkyl chains of the amphiphile are more tilted toward the surface. Assuming that the polyelectrolyte chain does not contribute significantly to the thickness, a tilt angle φ of ca. 50° is calculated (Table 6).

Conclusions

The poly(*p*-phenylenesulfonate)s (PPPS, PPPX) form complexes with dioctadecyldimethylammonium bromide (DODA) at the air/water interface. The structure of the complex monolayers is significantly different from that of pure DODA monolayers, in that the area per amphiphile is increased and can be correlated with the areal requirements of the polyelectrolyte in a stoichiometric complex. The stoichiometry of the complex was established by XPS measurements on LB films of the complexes. Thus, the aggregates of the poly(*p*-phenylene)s known to be present in the solution are not adsorbed as whole to form the complex with DODA at the air/water interface. This is further confirmed by X-ray reflectivity, which reveals a very smooth and well-defined layered structure for the LB films. The thickness of the layers is too small to accommodate aggregated poly(*p*-phenylene) chains. The X-ray reflectivity also reveals a strong tilt of the DODA alkyl chains of approximately 50°. Moreover, 1:1 stoichiometry and high regularity of the films can only be achieved by ordering of the rigid-rod-like PPPS in a two-dimensional nematic phase beneath the DODA monolayer. This nematic phase is the origin of the significant orientational order as indicated by polarized UV/vis spectroscopy on LB films. The degree of order shows a linear dependence on the molecular weight of the poly(*p*-phenylene) in the complex. Furthermore, the complex monolayer at the air/water interface has interesting UV/vis spectroscopic properties. A red shift of the poly(*p*-phenylene) A-band is observed compared to the corresponding solutions. Upon compression of the monolayer the peaks are red-shifted even further; thus, a piezochromic effect is observed. This effect is significant for PPPS (15 nm); however, it does not occur for the higher substituted PPPX. For PPPS an interesting dependence of the A-band peak position on the molecular weight is observed. As expected, in solution the A-band occurs at lower wavelength with decreasing degree of polymerization, since the conjugation length decreases. However, in the compressed monolayer the peak position is independent of the molecular weight. The piezochromic effect is discussed to be a result of $\pi-\pi$ interactions between the poly(*p*-phenylene) chains, which increase with decreasing distance during the compression.

Acknowledgment. We gratefully acknowledge the financial support by the Deutsche Forschungsgemeinschaft in their special program “Polyelectrolytes with defined molecular architecture” and by the Fonds der chemischen Industrie. We thank Dr. K. Schenck-Meuser and Prof. H. Duschner (Institut für Angewandte Struktur- und Mikroanalytik, Fachbereich Medizin, Johannes-Gutenberg-Universität Mainz) for performing XPS measurements. We thank Dr. M. Maskos and Prof. Dr. M. Schmidt (Institut für Physikalische Chemie, Johannes Gutenberg Universität Mainz) for MALDI-TOF spectrometry.

References and Notes

(1) Zhou, S.; Chu, B. *Adv. Mater.* **2000**, *12*, 545.
(2) Antonietti, M.; Burger, C.; Thünemann, A. *Trends Polym. Sci.* **1997**, *5*, 262.
(3) Ober, C. K.; Wegner, G. *Adv. Mater.* **1997**, *9*, 17.
(4) Erdelen, C.; Laschewsky, A.; Ringsdorf, H.; Schneider, J.; Schuster, A. *Thin Solid Films* **1989**, *180*, 153.
(5) Shimomura, M.; Kunitake, T. *Thin Solid Films* **1985**, *132*, 243.
(6) Engelking, J.; Ulbrich, D.; Meyer, W. H.; Schenk-Meuser, K.; Duschner, H.; Menzel, H. *Mater. Sci. Eng. C* **1999**, *8−9*, 29.
(7) Lackmann, H.; Engelking, J.; Menzel, H. *Mater. Sci. Eng. C* **1999**, *8−9*, 127.
(8) Nishiyama, K.; Fujihara, M. *Chem. Lett.* **1988**, 1257.
(9) Nishiyama, K.; Kurihara, M. A.; Fujihira, M. *Thin Solid Films* **1989**, *179*, 477.
(10) Sato, T.; Ozaki, Y.; Iriyama, K. *Langmuir* **1994**, *10*, 2363.
(11) Tachibana, H.; Azumi, R.; Tanaka, M.; Matsumoto, M.; Sako, S. I.; Sakai, H.; Abe, M.; Kondo, Y.; Yoshino, N. *Thin Solid Films* **1996**, *284−285*, 73.
(12) Niwa, M.; Mukai, A.; Higashi, N. *Langmuir* **1990**, *6*, 1432.
(13) Niwa, M.; Mukai, A.; Higashi, N. *Macromolecules* **1991**, *24*, 3314.
(14) Miyano, K.; Asano, K.; Shimomura, M. *Langmuir* **1991**, *7*, 444.
(15) Asano, K.; Miyano, K.; Ui, H.; Shimomura, M.; Ohta, Y. *Langmuir* **1993**, *9*, 3587.
(16) Morawetz, K.; Reiche, J.; Brehmer, L.; Jaeger, W. Presented at the 7th European Conference on Organized Films, ECOF7, 13.9−18.9, 1998, Potsdam, Germany.

(17) Engelking, J.; Wittemann, M.; Rehahn, M.; Menzel, H. *Langmuir* **2000**, *16*, 3407.
(18) Schnitter, M.; Engelking, J.; Heise, A.; Miller, R. D.; Menzel, H. *Macromol. Chem. Phys.* **2000**, *201*, 1504.
(19) Cimrová, V.; Remmers, M.; Neher, D.; Wegner, G. *Adv. Mater.* **1996** *8*, 146.
(20) Thünemann, A. F.; Ruppelt, D.; Schnablegger, H.; Blaul, J. *Macromolecules* **2000**, *33*, 2124.
(21) Rulkens, R.; Wegner, G.; Enkelmann, V.; Schulze, M. *Ber. Bunsen-Ges. Phys. Chem.* **1996**, *100*, 707.
(22) Loopinet, B.; Petekidis, G.; Fytas, G.; Rulkens, R.; Wegner, G.; *Langmuir* **1998**, *14*, 4958.
(23) Matsuyama, A.; Kishimoto, R.; Kato, T. *J. Chem. Phys.* **1997**, *106*, 6744.
(24) Rulkens, R.; Schulze, M.; Wegner, G. *Makromol. Rapid Commun.* **1994**, *15*, 669.
(25) Vanhee, S.; Rulkens, R.; Lehmann, U.; Rosenauer, C.; Schulze, M.; Köhler, W.; Wegner, G. *Macromolecules* **1996**, *29*, 5136.
(26) Räder, H. J.; Spickermann, J.; Kreyenschmidt, M.; Müllen, K. *Macromol. Chem. Phys.* **1996**, *197*, 3285.
(27) Menzel, H. *Macromol. Chem. Phys.* **1994**, *195*, 3747.
(28) Menzel, H.; Weichart, B.; Schmidt, A.; Paul, S.; Knoll, W.; Stumpe, J.; Fischer, T. *Langmuir* **1994**, *10*, 1926.
(29) Tajima, K.; Takahashi, M. *Thin Solid Films* **1989**, *178*, 381.
(30) Bonosi, F.; Gabrielli, G. *Colloids Surf.* **1991**, *52*, 277.
(31) Taylor, D. M.; Dong, Y.; Jones, C. C. *Thin Solid Films* **1996**, *284*, 130.
(32) Kozarac, Z.; Ahuja, R. C.; Möbius, D. *Langmuir* **1995**, *11*, 568.
(33) Kunitake, T. *Angew. Chem.* **1992**, *104*, 692.
(34) Engelking, J. Dissertation Universität, Hannover, Germany, 2000.
(35) Vahlenkamp, T. Dissertation, Universität Mainz, Germany, 1992.
(36) Ulbrich, D. Dissertation, Universität Mainz, Germany, 1999.
(37) Berndt, P.; Kurihara, K.; Kunitake, T. *Langmuir* **1992**, *8*, 2486.
(38) Vahlenkamp, T.; Wegner, G. *Makromol. Chem. Phys.* **1994**, *195*, 1933.
(39) Suzuki, H. *Bull. Chem. Soc. Jpn.* **1959**, *32*, 1340.
(40) Davydov, A. S. *Zh. Eks. Teor. Fiz.* **1948**, *18*, 515.
(41) Kuhn, W. *Helv. Chim. Acta* **1958**, *31*, 1780.
(42) Rehahn, M. Dissertation, Universität Mainz, Germany, 1990.
(43) Rehahn, M.; Schlüter, A.-D.; Wegner, G. *Makromol. Chem.* **1990**, *191*, 1991.
(44) Yoshida, M.; Nakanishi, F.; Seki, T.; Sakamoto, K.; Sakurai, H. *Macromolecules* **1997**, *30*, 1860.
(45) Weast, R. C.; Astle, M. J. *CRC Handbook of Chemistry and Physics*, 63th ed.; CRC Press: Boca Raton, FL, 1982.
(46) Laurence, C.; Nicolet, P.; Dalati, M. T.; Abboud, J.-M. M.; Notario, R. *J. Phys. Chem.* **1994**, *98*, 5807.
(47) Ochiai, K.; Tabuchi, Y.; Rikukawa, M.; Sanui, K.; Ogata, N. *Thin Solid Films* **1998**, *454*, 327.
(48) Bradley, D. D. C.; Grell, M.; Long, X.; Mellor, H.; Grice, A. *SPIE* **1997**, *3145*, 254.
(49) Fiesel, R.; Halkyard, C. E.; Rampey, M. E.; Kloppenburg, L.; Studer-Martinez, S. L.; Scherf, U.; Bunz, U. H. F. *Makromol. Rapid Commun.* **1999**, *20*, 107.
(50) Shimomura, M.; Ando, R.; Kunitake, T. *Ber. Bunsen-Ges. Phys. Chem.* **1983**, *87*, 1134.
(51) Kunitake, T. *Colloids Surf.* **1986**, *19*, 225.
(52) Shimomura, M.; Aiba, S.; Tagima, N.; Inoue, N.; Okuyama, K. *Langmuir* **1995**, *11*, 969.
(53) Kasha, M.; Rawls, H. R.; Ashraf El-Bayoumi, M. *Pure Appl. Chem.* **1965**, *11*, 371.
(54) Schwiegk, S.; Vahlenkamp, T.; Xu, Y.; Wegner, G. *Macromolecules* **1992**, *25*, 2513.
(55) Menzel, H.; Weichart, B.; Hallensleben, M. L. *Thin Solid Films* **1993**, *223*, 181.
(56) Menzel, H. In *The Polymeric Materials Encyclopedia: Synthesis, Properties and Applications*; Salamone, J. S., Ed.; CRC Press: Boca Raton, FL, 1996; p 2917.
(57) Khokhlov, A. R. In *Liquid Crystallinity in Polymers*; Ciferri, A., Ed.; VCH Pub.: New York, 1991; p 97.
(58) Khokhlov, A. R.; Semenov, A. N. *Macromolecules* **1986**, *19*, 373.
(59) Rulkens, R.; Wegner, G.; Thurn-Albrecht, T. *Langmuir* **1999**, *15*, 4022.
(60) Rulkens, R. Dissertation, Universität Mainz, Germany, 1996.
(61) Bockstaller, M.; Köhler, W.; Wegner, G.; Vlassopoulos, D.; Fytas, G.; Presented at the “BPS’99−Bayreuth Polymer & Materials Research Symposium: Polymeric Functional and Structural Materials” in Bayreuth, Germany, 1999.
(62) Higashi, N.; Kunitake, T. *Chem. Lett.* **1986**, 105.
(63) Although the X-ray reflectivity curves are well-resolved, it is not possible to fit the data. This is because the instrument did not allow to measure the edge of total reflection at very low angles.
(64) Essler, F. Dissertation, Universität Mainz, Germany, 1998.

MA0008140